Integrin β3 inhibition is a therapeutic strategy for supravalvular aortic stenosis

Ashish Misra,[1] Abdul Q. Sheikh,[1] Abhishek Kumar,[1] Jiesi Luo,[1] Jiasheng Zhang,[1] Robert B. Hinton,[3] Leslie Smoot,[4] Paige Kaplan,[5] Zsolt Urban,[6] Yibing Qyang,[1] George Tellides,[2] and Daniel M. Greif[1]

[1]Yale Cardiovascular Research Center, Section of Cardiovascular Medicine, Department of Internal Medicine and [2]Department of Surgery, School of Medicine, Yale University, New Haven, CT 06511
[3]Division of Cardiology, The Heart Institute, Cincinnati Children's Hospital Medical Center, Cincinnati, OH 45229
[4]Department of Cardiology, Boston Children's Hospital, Boston, MA 02115
[5]Section of Metabolic Diseases, Children's Hospital of Pennsylvania, Philadelphia, PA 19104
[6]Department of Human Genetics, Graduate School of Public Health, University of Pittsburgh, Pittsburgh, PA 15261

The aorta is the largest artery in the body, yet processes underlying aortic pathology are poorly understood. The arterial media consists of circumferential layers of elastic lamellae and smooth muscle cells (SMCs), and many arterial diseases are characterized by defective lamellae and excess SMCs; however, a mechanism linking these pathological features is lacking. In this study, we use lineage and genetic analysis, pharmacological inhibition, explant cultures, and induced pluripotent stem cells (iPSCs) to investigate supravalvular aortic stenosis (SVAS) patients and/or elastin mutant mice that model SVAS. These experiments demonstrate that multiple preexisting SMCs give rise to excess aortic SMCs in elastin mutants, and these SMCs are hyperproliferative and dedifferentiated. In addition, SVAS iPSC-derived SMCs and the aortic media of elastin mutant mice and SVAS patients have enhanced integrin β3 levels, activation, and downstream signaling, resulting in SMC misalignment and hyperproliferation. Reduced β3 gene dosage in elastin-null mice mitigates pathological aortic muscularization, SMC misorientation, and lumen loss and extends survival, which is unprecedented. Finally, pharmacological β3 inhibition in elastin mutant mice and explants attenuates aortic hypermuscularization and stenosis. Thus, integrin β3–mediated signaling in SMCs links elastin deficiency and pathological stenosis, and inhibiting this pathway is an attractive therapeutic strategy for SVAS.

The normal arterial wall is histologically divided into three layers: (1) an inner single layer of endothelial cells (ECs), (2) the media with alternating circumferential layers of smooth muscle and elastic lamellae, and (3) an outer adventitial layer, which includes fibroblasts and connective tissue. A critical component of the massive burden of cardiovascular disease on human health is an excessive and ectopic accumulation of arterial smooth muscle cells (SMCs). Unfortunately, therapeutic options for cardiovascular pathologies are hindered by our limited understanding of mechanisms underlying this vascular hypermuscularization (Owens et al., 2004; Seidelmann et al., 2014).

In diverse arterial diseases, such as atherosclerosis, restenosis, pulmonary hypertension, and supravalvular aortic stenosis (SVAS), excess SMCs are accompanied by defective elastic lamellae (Sandberg et al., 1981; Raines and Ross, 1993; Karnik et al., 2003). Elastin is a critical component of elastic lamellae, and heterozygous loss of function in the elastin gene (*ELN*) results in SVAS, a devastating human disease of excessively muscularized arteries (including the ascending and descending aorta; Curran et al., 1993; Li et al., 1998b; Pober et al., 2008). Major surgery is the only therapy for vessel obstruction in elastin arteriopathy. SVAS occurs as an isolated entity or more commonly as the major cause of morbidity in Williams-Beuren syndrome (WBS), which is caused by consecutive deletion of ∼26–28 genes, including *ELN*, on chromosome 7 (Pober et al., 2008). A mechanism linking elastin defects and hypermuscularization in SVAS or, for that matter, in any vascular disease is not delineated. Integrins are transmembrane receptors that link the extracellular matrix to the actin cytoskeleton and thus are candidates for mediating the effects of defective elastic lamellae on vascular smooth muscle; however, their role in elastin mutant arteriopathy has not been studied.

Here, we demonstrate that excess SMCs in elastin mutant mice derive from multiple preexisting SMCs that proliferate, dedifferentiate, and migrate. Integrin β3 expression, activation, and signaling are up-regulated in the aortic media of these mice and SVAS patients and in SVAS

Correspondence to Daniel M. Greif: daniel.greif@yale.edu

Abbreviations used: EC, endothelial cell; iPSC, induced pluripotent stem cell; PDGFR, platelet-derived growth factor receptor; pFAK, phosphorylated focal adhesion kinase; pH3, phosphohistone H3; Rb, Rainbow; SMA, α–smooth muscle actin; SMC, smooth muscle cell; SMMHC, smooth muscle myosin heavy chain; SVAS, supravalvular aortic stenosis; WBS, Williams-Beuren syndrome.

The Rockefeller University Press $30.00
J. Exp. Med. 2016 Vol. 213 No. 3 451–463
www.jem.org/cgi/doi/10.1084/jem.20150688

induced pluripotent stem cell (iPSC)–derived SMCs. Additionally, our results indicate that enhanced β3-mediated signaling is crucial for SMC misalignment and hyperproliferation in elastin mutants, and genetic or pharmacological inhibition of β3 in elastin mutant mice attenuates aortic hypermuscularization and stenosis. Furthermore, reducing the dosage of *Itgb3* (encoding β3) extends elastin-null survival; no prior interventions have increased the viability of elastin mutant mice. Hence, inhibiting integrin β3–mediated signaling in smooth muscle is an attractive pharmacological strategy for SVAS.

RESULTS

Multiple preexisting SMCs contribute to excess aortic smooth muscle in elastin mutants

We previously demonstrated that there is extensive SMC migration and mixing during the morphogenesis of the multilayered pulmonary artery but that hypoxia-induced distal pulmonary arteriole muscularization results from the clonal expansion of a single SMC marker$^+$ progenitor (Greif et al., 2012; Sheikh et al., 2015). Here, we initially investigated the cellular sources of excess SMCs in the elastin mutant model of SVAS and the clonal relationship of these pathological SMCs. The aortas of wild-type mice are not distinguishable from those of the $Eln^{(-/-)}$ or $Eln^{(+/-)}$ mutants until after embryonic day (E) 15.5 (Li et al., 1998a) or E18 (Wagenseil et al., 2010), respectively. After E15.5, arteries and arterioles of $Eln^{(-/-)}$ embryos and early postnatal mice accumulate excess SMCs on the endothelial side of the media (mimicking human SVAS), which ultimately obstruct the lumen and result in death by the initial postnatal days (Li et al., 1998a). In contrast, between E18 and birth, the outer aspect of the $Eln^{(+/-)}$ aortic media accumulates additional lamellar units, whereas the wild-type aortic structure does not change (Li et al., 1998b). We induced dams pregnant with *α–smooth muscle actin* (*SMA*)-*CreER*^{T2}, *ROSA26R*$^{(mTmG/+)}$ embryos (Muzumdar et al., 2007; Wendling et al., 2009) that were also either mutant or wild type for the elastin gene with a single tamoxifen dose (1.5 mg) at E12.5 and analyzed newborns at postnatal day (P) 0.5. Many of the excess SMCs in elastin mutants—inner medial SMCs in $Eln^{(-/-)}$ newborns and outer layer SMCs in $Eln^{(+/-)}$ newborns—were GFP$^+$ (51 ± 3% and 41 ± 3%, respectively), indicating that they derive from SMCs present at the time of marking (Fig. 1 A). In contrast, EC fate mapping in *Cdh5-CreER*^{T2} mice (Wang et al., 2010) also carrying $Eln^{(-/-)}$ and *ROSA26R*$^{(mTmG/+)}$ indicates that ECs do not contribute to the excess SMCs in elastin nulls (unpublished data). Furthermore, we induced $Eln^{(-/-)}$, *SMA-CreER*^{T2} embryos also carrying the multi-color Rainbow (Rb) Cre reporter *ROSA26R*$^{(Rb/+)}$ with a single tamoxifen injection at E12.5. At E18.5, these embryos were found to have SMCs of multiple colors in the inner layers of the aorta (Fig. 1 B). Thus, excess aortic SMCs in elastin-null mice derive from multiple preexisting SMCs.

Excess proliferation and smooth muscle myosin heavy chain (SMMHC) down-regulation in the elastin mutant aorta

The mechanisms underlying the different phenotypes of the elastin-null or heterozygous aorta are not delineated. It has previously been reported that the late embryonic $Eln^{(-/-)}$ aorta has more proliferating SMCs than the wild type aorta, predominantly in the inner layers (Li et al., 1998a). We found that in comparison to wild type, the number of SMCs staining for the proliferation markers phosphohistone H3 (pH3) or Ki67 was increased three- to fourfold in the $Eln^{(-/-)}$ aorta at E17.5 (Fig. 2, A–D) and 1.7-fold in the $Eln^{(+/-)}$ aorta at E18.5 (Fig. 2, E–H). Interestingly, the increased proliferation of the $Eln^{(+/-)}$ aortic SMCs predominantly results from cells in the outermost smooth muscle layer (Fig. 2, E–H). In addition to excessive migration and proliferation, the $Eln^{(-/-)}$ aortic media has markedly reduced expression of the canonical SMC differentiation marker SMMHC (Miano et al., 1994) at P0.5 (Fig. 3, A and B) but no appreciable change in expression of markers of early SMCs (SMA and SM22-α; not depicted) or undifferentiated mesenchyme (platelet-derived growth factor receptor [PDGFR]–β; Fig. 3, C and D).

Enhanced integrin β3 signaling in mouse and human elastin mutant aorta

Our findings indicate that elastin mutant SMCs are hyperproliferative, undifferentiated and migrate radially; however, the underlying signaling pathways are not defined. We investigated integrins because they are implicated in filopodia-mediated cell migration (Arjonen et al., 2011), and we observed increased filopodia-like projections in elastin mutant SMCs (see Fig. 1 A, close-ups). We initially found markedly increased expression of integrins β3 and β1 in the elastin mutant aortic wall (Fig. 4, A–E). In $Eln^{(-/-)}$ mice, there is increased expression of β3 in subendothelial SMC layers, and β1 in ECs and many outer layer SMCs. In the human aorta, β3 is markedly up-regulated in the media of patients with WBS (Fig. 4 F) and SVAS (not depicted). In addition, iPSCs derived from coronary artery SMCs of a SVAS patient or control human (Ge et al., 2012) express equivalent low levels of β3 protein (not depicted); however, when converted into SMCs, SVAS iPSC-SMCs (Ge et al., 2012) have robust up-regulation of β3 protein in comparison with control iPSC-SMCs (Fig. 4, G and H).

Beyond enhanced expression, we next assessed integrin signaling. The aortic media of both humans with WBS and $Eln^{(-/-)}$ mice has enhanced staining with the WOW-1 antibody, which recognizes activated αvβ3 (Pampori et al., 1999; Fig. 5, A and B). In addition, phosphorylated focal adhesion kinase (pFAK), a downstream regulator of integrin signaling (Fig. 5 C) is up-regulated in the elastin-null mouse aorta. Finally, the expression of the β1 and β3 ligand fibronectin is increased in the elastin-null mouse aorta (Fig. 5 D), whereas the pattern of collagen IV expression is unchanged (not depicted). Collectively, our results suggest that β3-mediated signaling is up-regulated in the aortic media of elastin mutant mice and humans.

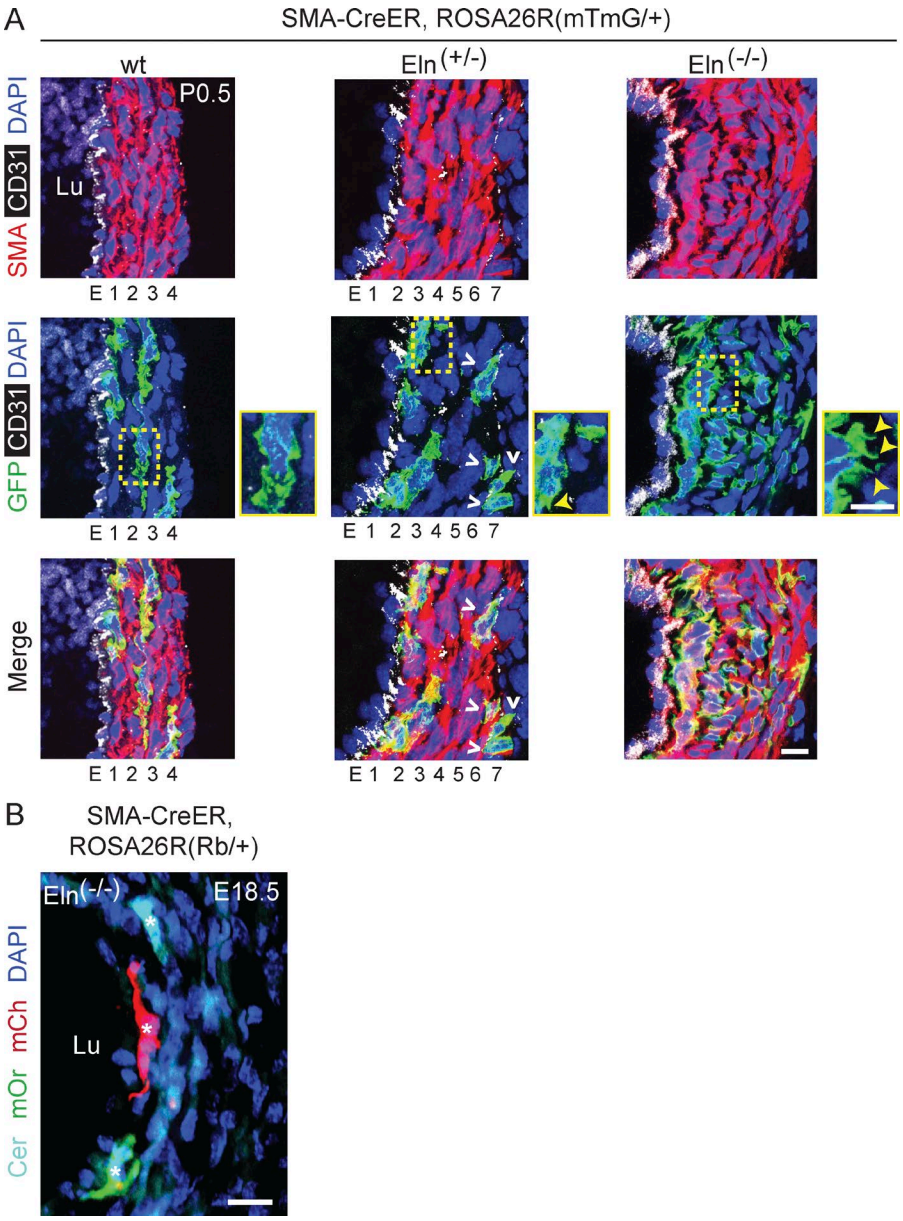

Figure 1. **Multiple preexisting SMCs give rise to excess smooth muscle in elastin mutants.** Transverse descending aortic sections of *SMA-CreER*^{T2} mice also carrying *ROSA26R*$^{(mTmG/+)}$ (A) or *ROSA26R*$^{(Rb/+)}$ (B) and of the indicated elastin genotype induced with tamoxifen at E12.5. (A) Sections at P0.5 were stained for SMA, GFP (lineage marker), CD31, and nuclei (DAPI), and GFP$^+$ SMCs are included in extra aortic wall layers in *Eln*$^{(+/-)}$ (outer layer; open arrowheads) and in *Eln*$^{(-/-)}$ (inner layer adjacent to endothelium). The boxed regions are shown as close-ups with closed arrowheads indicating increased SMC projections in elastin mutants. (B) Section at E18.5 was analyzed with direct fluorescence of Rb colors and staining for DAPI. Excess inner layer SMCs of *Eln*$^{(-/-)}$ aorta include cells of multiple colors (asterisks) indicating polyclonality. For each genotype, $n = 4$ pups in A and $n = 3$ embryos in B. Lu, aortic lumen; E, endothelial layer; 1–7, smooth muscle layers. Bars, 10 µm.

Reduced integrin β3 attenuates aortic hypermuscularization and extends viability of elastin nulls

To test the hypothesis that enhanced β3-dependent signaling plays a key role in subendothelial SMC accumulation in elastin nulls, we investigated the effect of reducing the dosage of the gene encoding β3, *Itgb3*, on the *Eln*$^{(-/-)}$ aortic phenotype and viability. Importantly, wild-type and *Itgb3* mutant (Hodivala-Dilke et al., 1999) aortas are not distinguishable (unpublished data). In the background of the elastin-null genotype, mutants that are *Itgb3*$^{(+/-)}$ or *Itgb3*$^{(-/-)}$ have markedly attenuated hypermuscularization and stenosis of the aorta compared with mice wild type for *Itgb3* (Fig. 6, A–C). Many SMCs of the inner layers of the early postnatal *Eln*$^{(-/-)}$ aorta are misaligned (Li et al., 1998a; Wagenseil et al., 2009) as shown in Fig. 6 D, oriented radially instead of circumferentially. As integrins influence mitotic spindle orientation and thus the division axes of diverse cell types (Streuli, 2009), we postulated that β3 up-regulation in the elastin mutant aortic media plays a crucial role in shifting SMC orientation and migration direction, contributing to the increased smooth muscle layers and disarray. Indeed, our experiments indicate that reduction of the *Itgb3* gene dosage of *Eln*$^{(-/-)}$ mutants prevents inner layer aortic SMCs from assuming an abnormal radial orientation and instead preserves their circumferential orientation (Fig. 6, D and E). In addition, reduction of the *Itgb3* gene dosage substantially lessens the excess proliferation of *Eln*$^{(-/-)}$ aortic SMCs (Fig. 6 F) but does not augment SMMHC expression (not depicted). Moreover, the survival

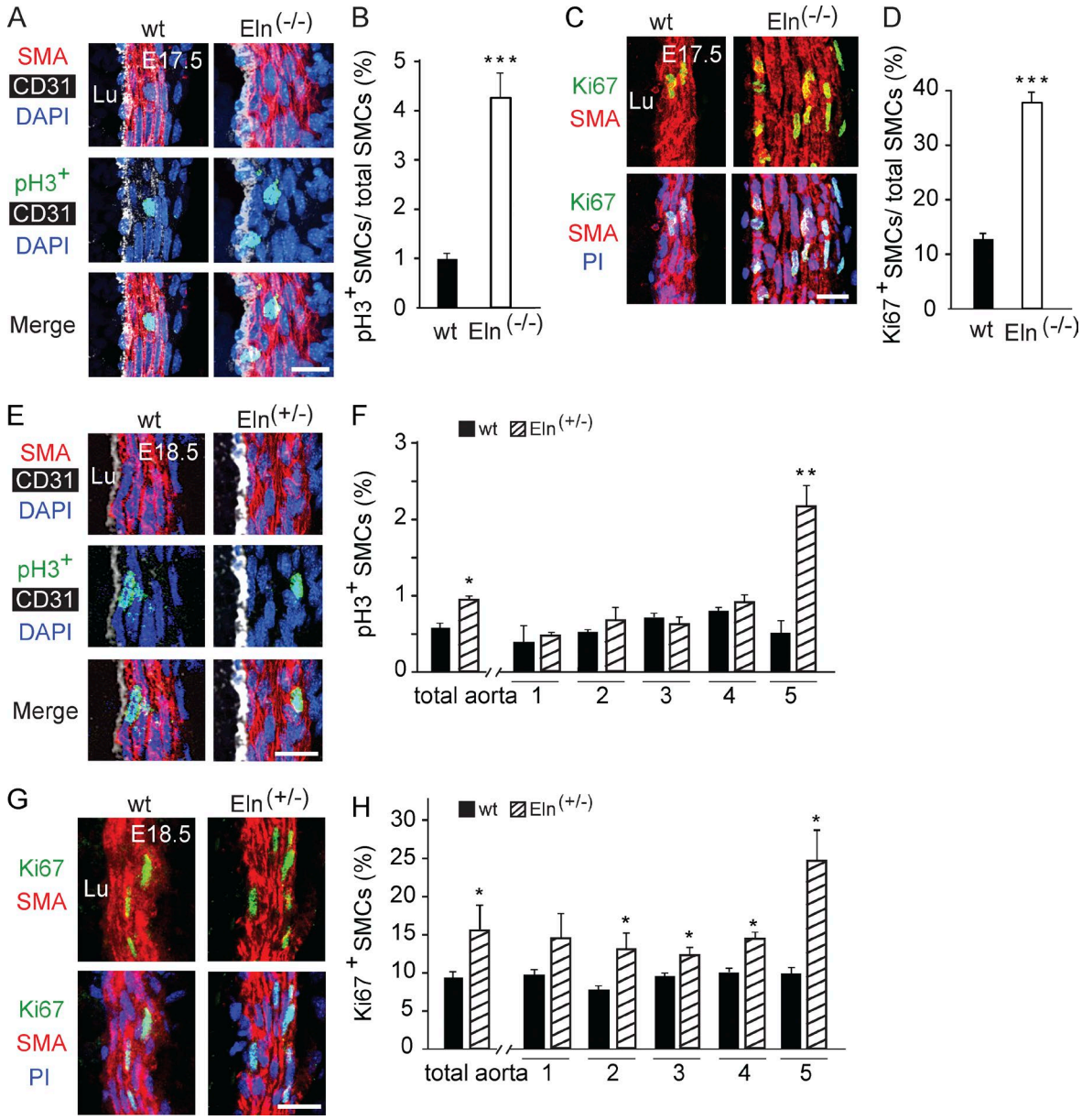

Figure 2. **SMC hyperproliferation in elastin mutant aorta.** (A, C, E, and G) Transverse aortic sections of embryos of the indicated elastin genotype and age stained for SMA and nuclei and for either pH3 (A and E) or Ki67 (C and G). Nuclei are stained with DAPI (A and E) or propidium iodide (PI; C and G). Staining for CD31 is also included in A and E. (B, D, F, and H) Proliferative index (fraction of pH3$^+$ or Ki67$^+$ cells) of SMCs of wild-type, *Eln*$^{(+/-)}$, and/or *Eln*$^{(-/-)}$ embryos at E17.5 (B and D) or E18.5 (F and H) in the total aorta and, for F and H, in each cell layer (i.e., layers 1–5; this analysis was limited to aortic sections with five smooth muscle layers). For each genotype, $n = 3$ embryos in B and H and $n = 2$ embryos in D and F, and 20 sections per embryo were analyzed. The total pH3$^+$ aortic SMCs detected in B were 172 for wild type and 787 for *Eln*$^{(-/-)}$ and in F were 71 for wild type and 133 for *Eln*$^{(+/-)}$, whereas the total Ki67$^+$ SMCs detected in D were 1,389 for wild type and 4,785 for *Eln*$^{(-/-)}$ and in H were 1,765 for wild type and 3,357 for *Eln*$^{(+/-)}$. Data are presented as mean ± SD. Student's *t* test was used. *, $P < 0.05$; **, $P < 0.01$; ***, $P < 0.001$ versus wild type. Lu, aortic lumen. Bars, 10 µm.

of elastin nulls is extended by reducing *Itgb3* gene dosage (Fig. 6 G), which is without precedent.

Pharmacological inhibition of β3 in elastin mutant mice blocks aortic muscularization and stenosis

Given that reducing *Itgb3* gene dosage attenuates the *Eln*$^{(-/-)}$ aortic phenotype, we next evaluated whether pharmacological inhibition of β3 in tissue culture or in vivo has a similar effect. Li et al. (1998a) previously demonstrated that *Eln*$^{(-/-)}$ embryonic aortic explants become completely stenosed within 1 d in culture, and wild-type explants remain patent. We harvested aortas from wild-type or *Eln*$^{(-/-)}$ embryos at E15.5 and cultured explants for 18 h in the presence of an anti-β3 blocking antibody (Lawler et al., 1988; Scheppke et

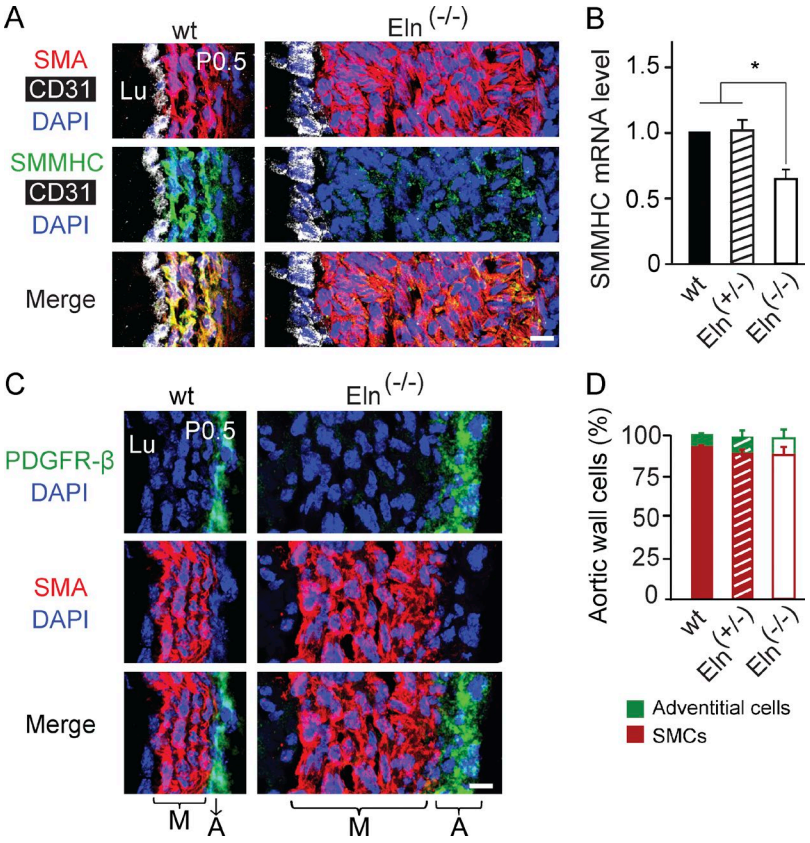

Figure 3. **Dedifferentiation of aortic SMCs in elastin nulls.** (A) Transverse aortic sections of wild-type and *Eln*$^{(-/-)}$ pups at P0.5 were stained for SMA, SMMHC, CD31, and nuclei (DAPI). (B) SMMHC mRNA levels normalized to *Gapdh* as measured by RT-PCR from aortas of specified genotype at P0.5; $n = 3$ aortas in duplicate. (C) Aortic sections of pups as in A were stained for SMA, PDGFR-β, and DAPI. At P0.5, PDGFR-β marks outer layer SMA$^-$ cells (i.e., adventitial cells). Note the hyperplasia of both smooth muscle and adventitia of the elastin-null aorta. (D) Cells (DAPI$^+$ nuclei) of descending aortic wall of the specified elastin genotypes were scored as SMCs (PDGFR-β$^-$SMA$^+$) or adventitial cells (PDGFR-β$^+$SMA$^-$). The total numbers of scored cells were 528, 584, and 778 for wild type, *Eln*$^{(+/-)}$, and *Eln*$^{(-/-)}$, respectively. For each genotype, $n = 3$ pups. Data are presented as mean ± SD. ANOVA was used. *, $P < 0.05$. Lu, aortic lumen; M, media; A, adventitia. Bars, 10 µm.

al., 2012) or IgG1 isotype control. β3 blockade attenuated lumen loss and medial wall area expansion in *Eln*$^{(-/-)}$ aortic explants (Fig. 7, A–C) but did not have a substantial effect in wild-type explants (not depicted). For in vivo experiments, we used the β3 and β5 inhibitor cilengitide, which has been tested in humans as a therapy for glioblastoma multiforme (Dechantsreiter et al., 1999; Stupp et al., 2014). *Eln*$^{(+/-)}$ males and females were mated, and a miniature osmotic pump containing cilengitide or vehicle was implanted in each pregnant dam at E13.5 for continuous infusions because cilengitide has a short half-life in plasma. At P0.5, we genotyped and euthanized pups and analyzed their aortas. Cilengitide treatment does not alter aortic SMC orientation, muscularization, or lumen size of wild-type mice. However, in elastin nulls, cilengitide substantially preserves SMC circumferential orientation and attenuates aortic hypermuscularization and stenosis (Fig. 7, D–H). Similarly, cilengitide treatment of *Eln*$^{(+/-)}$ mice prevents enhanced muscularization (6.9 ± 0.2 smooth muscle layers at P0.5 with PBS treatment vs. 4.4 ± 0.2 layers with cilengitide treatment; $n = 3$; $P < 0.005$) and preserves lumen size (Fig. 7, D–F). Collectively, our findings establish a novel link between elastin deficiency, integrin β3, and arterial hypermuscularization.

DISCUSSION

SVAS, a morbid disease caused by heterozygous loss-of-function mutations in the *ELN* gene, is characterized by excessive smooth muscle and occlusions in large caliber arteries, such as the aorta. SVAS occurs alone or more commonly as part of WBS, and collectively, it afflicts approximately 1 in 5,000 individuals. The only current therapy for this aortic obstruction is major vascular surgery, which carries a substantial risk of morbidity and mortality. Undoubtedly, there is a strong need for investigations into the cellular and molecular mechanisms underlying the pathogenesis of elastin arteriopathy, which, in turn, promise to yield novel therapeutic strategies.

In addition to SVAS, the accumulation of excess and ectopic SMCs is a key component of many other vasculoproliferative diseases, and the cellular origins of these pathological SMCs are beginning to be defined. We and others have shown that preexisting SMCs contribute to hypermuscularization in atherosclerosis, arterial injury, and pulmonary hypertension (Feil et al., 2004; Herring et al., 2014; Sheikh et al., 2014, 2015; Shankman et al., 2015). In addition, ECs are implicated as a source of vascular SMCs in development and disease (DeRuiter et al., 1997; Yamashita et al., 2000; Arciniegas et al., 2007; Morimoto et al., 2010; Chen et al., 2012; Qiao et al., 2014; Ranchoux et al., 2015), yet no prior studies have lineage traced any cell population in elastin mutants. Our fate mapping and clonal analyses demonstrate that multiple excess SMCs in the elastin mutant aorta derive from preexisting SMCs (Fig. 1) but not ECs. Interestingly, the outward radial migration of SMCs contributes to the construction of outer smooth muscle layers during both morphogenesis of the nor-

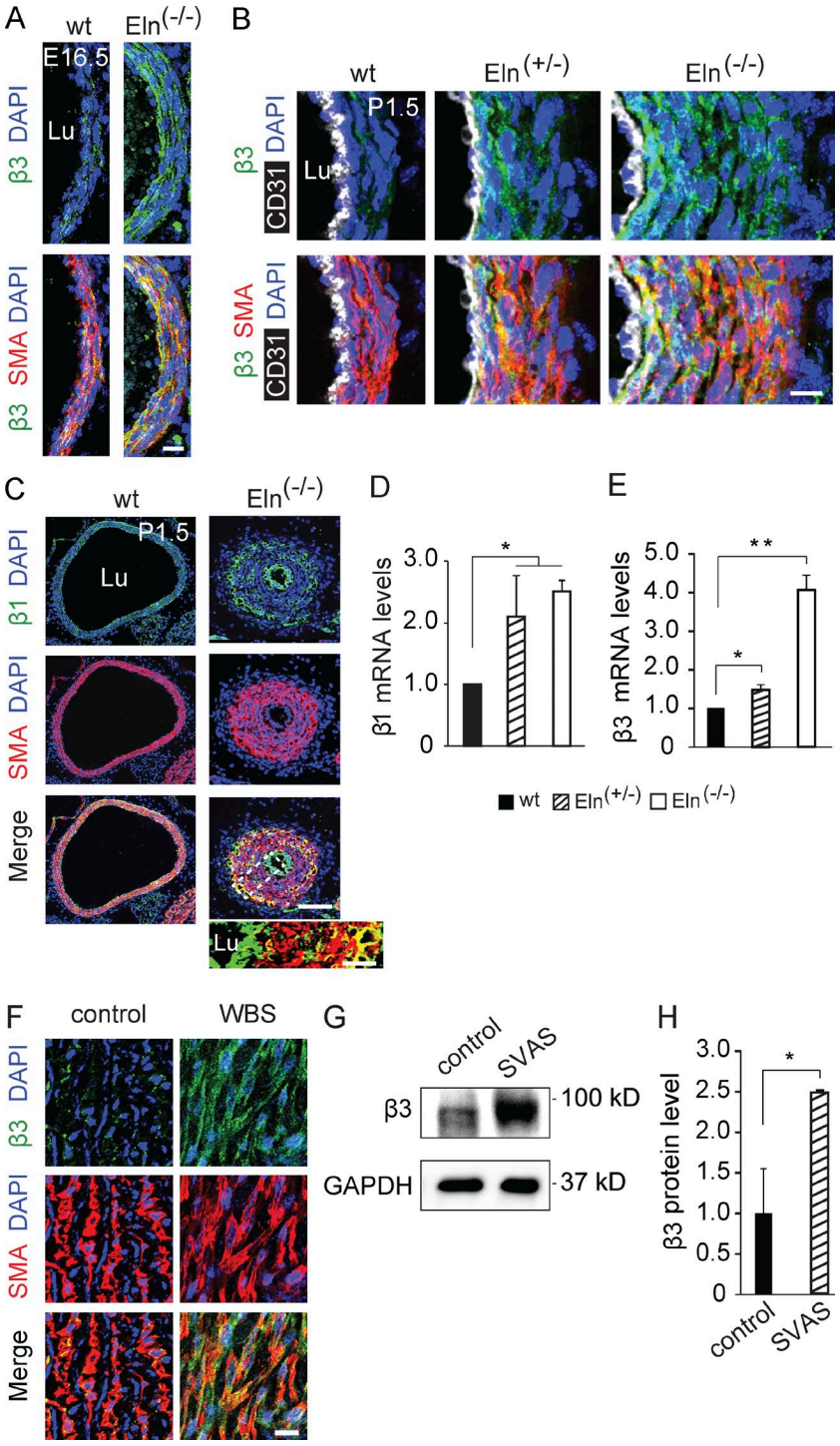

Figure 4. **Increased β integrin expression in the human and mouse elastin mutant aorta.** (A–C) Transverse aortic sections of wild-type and elastin mutant littermates at E16.5 or P1.5 stained for SMA and nuclei (DAPI) and for either integrin β3 (A and B) or β1 (C). CD31 staining is also included in B. The boxed region of $Eln^{(-/-)}$ aorta in C is shown as an inset without DAPI staining. Note that β3 expression is increased in the SMCs of the *Eln* mutant aortas, particularly in subendothelial layers of $Eln^{(-/-)}$, and β1 expression is up-regulated in ECs and many SMCs, primarily in the outer smooth muscle layers in $Eln^{(-/-)}$ aorta. For each genotype, $n = 3$ pups in A and C and $n = 4$ pups in B. (D and E) β1 and β3 transcript levels normalized to *Gapdh* as measured by qRT-PCR of cDNAs from aortas of specified elastin genotype at P0.5; $n = 3$ in duplicate. (F) Representative images of aortic sections of WBS patients (age 5 mo) and age-matched human controls stained for SMA, activated β3, and nuclei (DAPI); $n = 3$ patients. SVAS is the major cause of morbidity in WBS patients. (G and H) Protein levels of β3 and GAPDH in iPSC-SMCs derived from SVAS or control patients were assayed by Western blot with densitometric analysis of β3 normalized to GAPDH; $n = 2$. Data are presented as mean ± SD. ANOVA was used in D and E, and Student's *t* test in H. *, $P < 0.05$; **, $P < 0.01$. Lu, aortic lumen. Bars: (A, B, F, and inset in C) 10 µm; (main images in C) 100 µm.

mal pulmonary artery (Greif et al., 2012) and pathogenesis of the $Eln^{(+/-)}$ aorta (Fig. 1).

Elastin mutant arteries are hypermuscular with additional smooth layers forming on the outer aspect of the $Eln^{(+/-)}$ media and excess SMCs accumulating on the inner aspect of the $Eln^{(-/-)}$ media (Li et al., 1998a,b). Mechanisms underlying these different radial locations of excessive smooth muscle are not established. Our findings suggest that the different locations of enhanced SMC proliferation in $Eln^{(+/-)}$ (outer layer SMCs; Fig. 2) and $Eln^{(-/-)}$ (inner layer SMCs; Li et al., 1998a) aortas are likely to be key factors underlying the different phenotypes of these genotypes.

Because elastin mutants have an altered extracellular matrix, including increased vessel fibronectin (Fig. 5), and

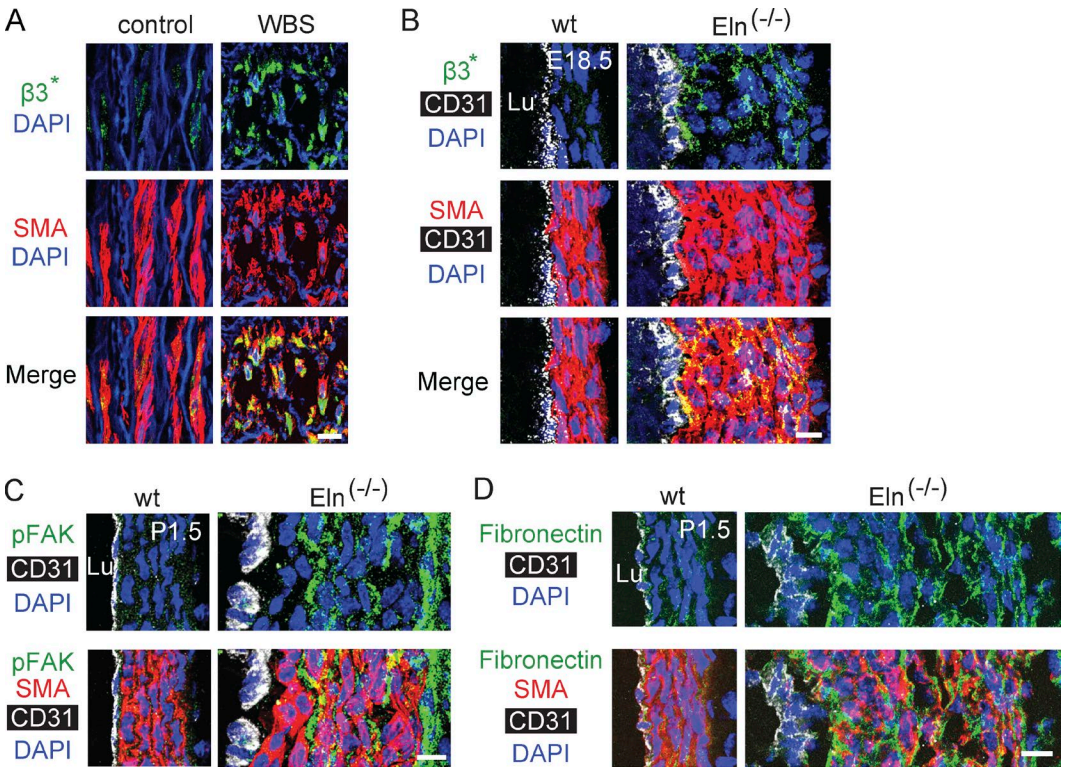

Figure 5. **Enhanced integrin signaling in elastin mutants.** (A) Aortic sections of WBS patient (age 46 yr) and age-matched human control stained for SMA, activated β3, and nuclei (DAPI); $n = 3$ patients. Asterisks signify activated integrin β3. (B–D) Transverse aortic sections of wild-type and $Eln^{(-/-)}$ littermates at E18.5 or P1.5, stained for CD31, SMA, and nuclei (DAPI), and for either activated β3 (B), pFAK (C), or fibronectin (D). For each genotype, $n = 3$ mice. Lu, aortic lumen. Bars, 10 µm.

integrins link the extracellular matrix to intracellular signaling pathways, we reasoned that integrins may be critical in the resulting arterial disease. Karnik et al. (2003) previously suggested that integrins are not involved in elastin-mediated signaling as calcium chelation did not impact tropoelastin-induced migration or actin polymerization in cultured $Eln^{(-/-)}$ SMCs. Our findings in human and mouse aortas demonstrate that elastin mutants have up-regulated integrin β3 expression, activation, and signaling, and interestingly, in the $Eln^{(-/-)}$ aorta, β3 expression is highest in SMCs of the inner layers, where many cells are misoriented (Figs. 4 and 6). We have previously demonstrated that iPSC-SMCs generated from SVAS or WBS patients are more proliferative and migratory than control iPSC-SMCs (Ge et al., 2012), and herein, we show that SVAS iPSC-SMCs have robustly up-regulated expression of integrin β3 protein (Fig. 4). Moreover, genetic or pharmacological β3 inhibition in $Eln^{(-/-)}$ mice and explants prevents aortic hypermuscularization and stenosis and SMC misorientation (Figs. 6 and 7). Because our in vivo pharmacological experiments use cilengitide, which is a strong inhibitor of αvβ3 but also has anti-αvβ5 activity, further histological and genetic studies will characterize β5 expression and the effect of specific *Itgb5* deletion in elastin mutants. Integrins are key players in regulating cell shape and division axis (Streuli, 2009), and we posit that SMC proliferation and radial migration is limited by the circumferential orientation of maturing wild-type SMCs, whereas the pathological radial orientation of $Eln^{(-/-)}$ SMCs is permissive.

Our findings of the role of integrin β3 in elastin mutant aortopathy should be considered in the context of prior investigations of β3 in atherosclerosis and vascular injury. β3 is expressed in the human coronary artery media (Hoshiga et al., 1995) and in SMCs of the neointima of atherosclerotic or mechanically injured arteries (Hoshiga et al., 1995; Stouffer et al., 1998). Treatment of diabetic pigs with an anti-β3 antibody attenuates atherosclerotic lesion formation (Maile et al., 2010), and after carotid artery ligation, $Itgb3^{(-/-)}$ mice have reduced neointimal size and SMC accumulation (Choi et al., 2004). In contrast, global knockout of *Itgb3* worsens atherosclerotic burden in $ApoE^{(-/-)}$ mice fed a high-fat diet (Weng et al., 2003). This worsening likely results from the effects of nonsmooth muscle bone marrow–derived cells (e.g., macrophages) as $Itgb3^{(+/+)}$, $LDLR^{(-/-)}$ mice have accelerated atherosclerosis when transplanted with $Itgb3^{(-/-)}$, $LDLR^{(-/-)}$ bone marrow (Schneider et al., 2007). We conjecture that, similar to our hypothesis for elas-

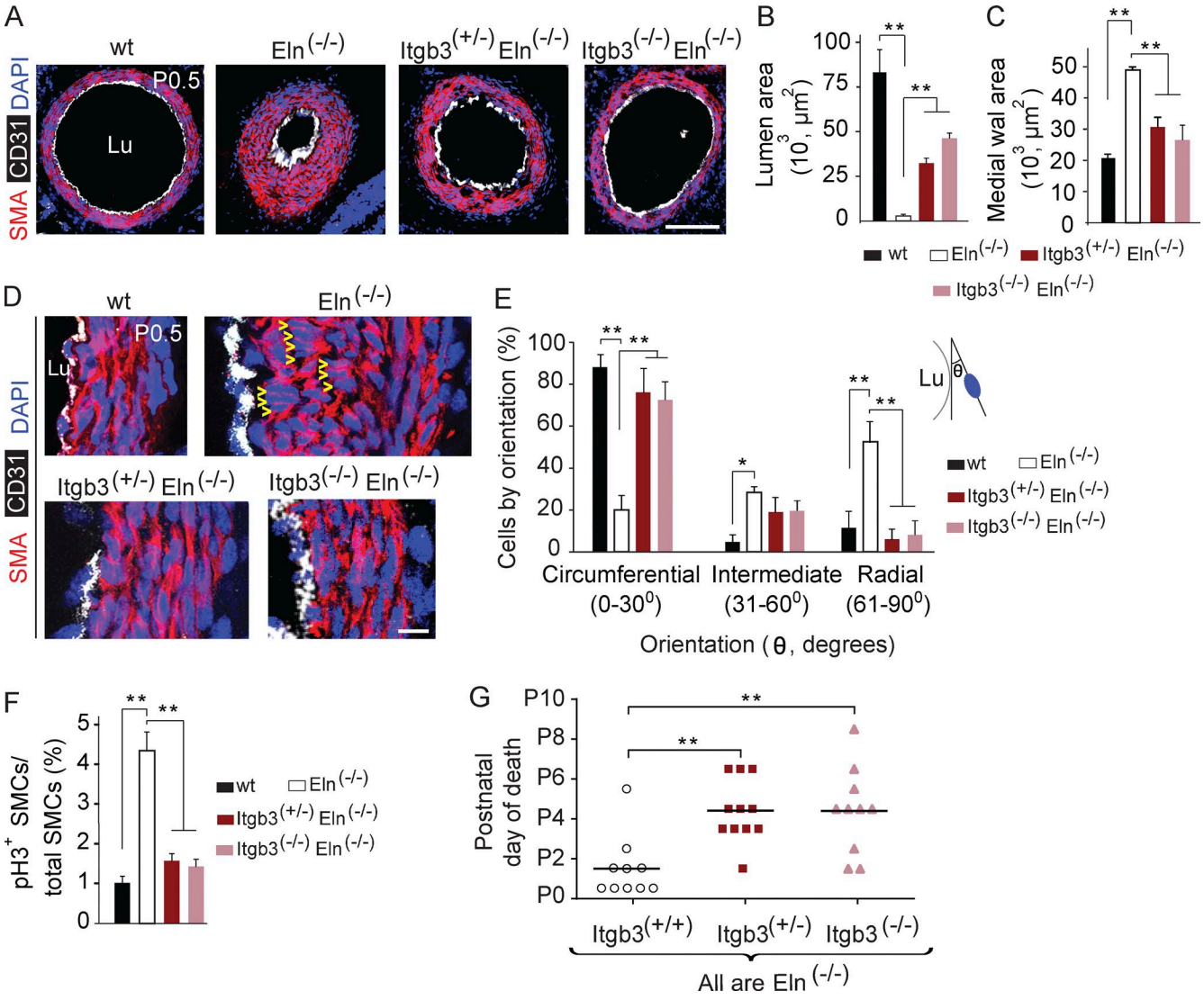

Figure 6. **Reduced integrin β3 gene dosage inhibits aortic hypermuscularization and extends viability of elastin nulls.** (A) Transverse descending aortic sections of newborns of indicated genotype at P0.5 were stained for SMA, CD31, and nuclei (DAPI). (B and C) Aortic lumen and medial wall area were determined from sections as shown in A; $n = 3$ aortas per genotype, 3 sections per aorta. Note that reduced *Itgb3* dosage attenuates $Eln^{(-/-)}$ aortic hypermuscularization. (D) Sections cut and stained as in A with high power magnification of the aortic wall demonstrating that wild-type SMCs are circumferentially oriented, whereas the abnormal radial orientation of SMCs in the inner layers of the $Eln^{(-/-)}$ aorta is prevented by reducing *Itgb3* dosage. Arrowheads indicate examples of radially oriented SMCs in $Eln^{(-/-)}$ aorta. (E) Quantification of nuclear orientation of cells in inner three aortic smooth muscle layers of embryos of the indicated genotype at P0.5 with respect to the tangent of the lumen boundary; $n = 3$ aortas, and >200 SMCs were scored for each genotype. (F) Proliferative index (fraction of $pH3^+$ cells) of aortic SMCs of embryos of the indicated genotype at E17.5. 20 sections per embryo were analyzed, and the number of embryos analyzed and $pH3^+$ aortic SMCs detected were 3 embryos and 172 SMCs for wild type, 3 and 787 for $Eln^{(-/-)}$, 2 and 184 for $Itgb3^{(+/-)}$ $Eln^{(-/-)}$, and 2 and 163 for $Itgb3^{(-/-)}Eln^{(-/-)}$. (G) The age of death of each $Eln^{(-/-)}$ newborn is classified by *Itgb3* genotype, with bars indicating the mean age of death. Reduced *Itgb3* gene dosage increases viability of elastin-null pups. Data are presented as mean ± SD. ANOVA was used. *, $P < 0.05$; **, $P < 0.01$. Lu, aortic lumen. Bars: (A) 100 µm; (D) 10 µm.

tin mutants, in other vasculoproliferative disorders, altered β3-mediated signaling in SMCs changes cell orientation, allowing for aberrant proliferation and migration.

Finally, we observed that reduction in *Itgb3* gene dosage extends the survival of $Eln^{(-/-)}$ mutants (Fig. 6), which is unprecedented for any previous intervention. This increased viability is limited to ∼3 d, likely because of defects in tissues beyond the aorta, such as the lung parenchyma. Indeed, mice with ∼35% of the normal elastin levels have abnormal lung development, resulting in congenital emphysema (Shifren et al., 2007). Importantly, however, SVAS patients (heterozygotes for the *ELN*-null allele) lack a lung

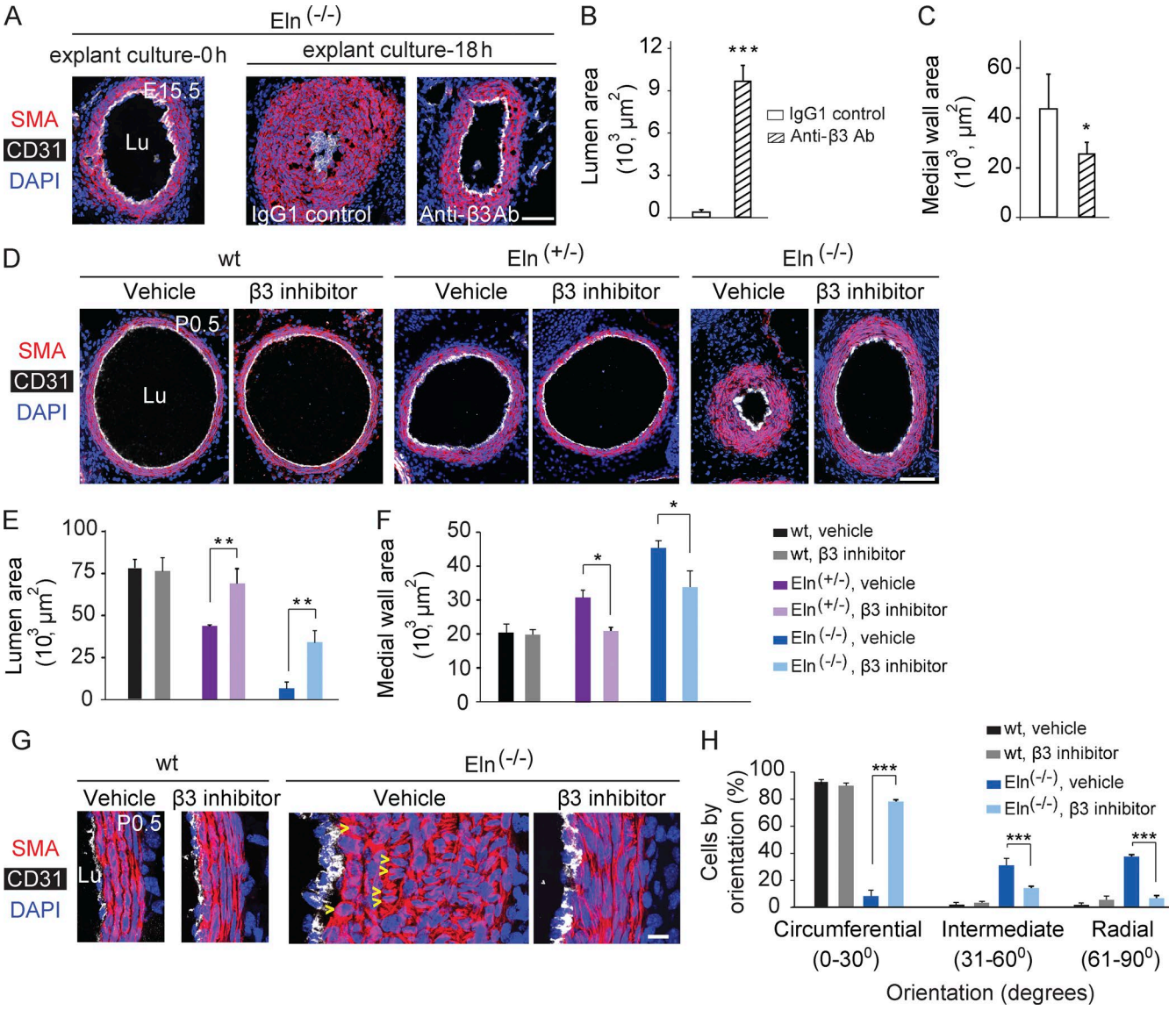

Figure 7. **Pharmacological blockade of β3 attenuates *Eln*$^{(-/-)}$ aortic hypermuscularization and stenosis.** (A) Aortas were harvested from *Eln*$^{(-/-)}$ embryos at E15.5 and fixed either immediately or after culturing as explants for 18 h in the presence of an isotype control IgG1 or an integrin αvβ3–blocking antibody. Transverse sections were stained for SMA, CD31, and nuclei (DAPI). (B and C) *Eln*$^{(-/-)}$ aortas cultured for 18 h and sectioned and stained as in A were used to calculate the lumen and media wall areas; $n = 3$ aortas, 3 sections per aorta. (D–H) Female and male *Eln*$^{(+/-)}$ mice were crossed, and pregnant dams were implanted with miniature osmotic pumps containing integrin β3 inhibitor cilengitide or vehicle (PBS) at E13.5. (D) Transverse aortic sections of wild-type, *Eln*$^{(+/-)}$, and *Eln*$^{(-/-)}$ pups at P0.5 were stained as in A and used to measure lumen and media wall area as shown in E and F; $n = 3$ aortas per genotype, 3 sections per aorta. (G) High magnification images of vehicle- or cilengitide-treated wild-type and *Eln*$^{(-/-)}$ aortas at P0.5 were sectioned and stained as in A, and arrowheads indicate examples of radially oriented SMCs. These images were used to quantify the SMC nucleus orientation in the inner three layers of aortic media (H); per each genotype + cilengitide/vehicle group, $n = 3$ aortas, and >275 SMCs were scored. Data are presented as mean ± SD. ANOVA was used. *, $P < 0.05$; ** $P < 0.01$; ***, $P < 0.001$. Lu, aortic lumen. Bars: (A and D) 100 µm; (G) 10 µm.

phenotype (Li et al., 1998b; Pober et al., 2008) and thus may greatly benefit from the favorable vascular effects of anti-β3 therapy. In summary, our findings indicate that enhanced integrin β3 signaling is a crucial link between elastin deficiency and arterial hypermuscularization, and β3 blockade is a promising and much needed noninvasive therapeutic approach for SVAS.

MATERIALS AND METHODS

Animals. All mouse experiments were approved by the Institutional Animal Care and Use Committee at Yale University. Wild-type C57BL/6, *ROSA26R*$^{(mTmG/mTmG)}$, and *Itgb3*$^{(+/-)}$ mice were purchased from The Jackson Laboratory (Hodivala-Dilke et al., 1999; Muzumdar et al., 2007). *SMA-CreER*^{T2}, *Cdh5-CreER*^{T2}, *ROSA26R*$^{(Rb/Rb)}$, and *Eln*$^{(+/-)}$ mice have

been described previously (Li et al., 1998a; Wendling et al., 2009; Wang et al., 2010; Rinkevich et al., 2011). *Itgb3*$^{(+/-)}$, *Eln*$^{(+/-)}$, and *CreER* mice were maintained on the C57BL/6 background. For timed pregnancies, noon of the day of vaginal plug detection was designated as E0.5, and embryos were dissected in PBS.

Aortic explant culture. Descending aortas were dissected from mouse embryos at E15.5 and cultured for 18 h at 37°C in 0.5% FBS in DMEM with either an anti-αvβ3 integrin blocking antibody (1:50; BD) or an isotype control IgG1.

Immunohistochemistry. Mouse tissue was fixed with 4% paraformaldehyde and then incubated in 30% sucrose, embedded in optical cutting temperature compound (Tissue Tek), and stored at −80°C. All immunohistochemical analysis of mouse tissue was conducted on the proximal thoracic descending aorta (the initial 1.5 mm) immediately distal to the aortic arch. Frozen tissue was cryosectioned (10 µm) in the transverse axis, and sections were incubated with blocking solution (5% goat serum in 0.1% Triton X-100 in PBS [PBS-T]) and then with primary antibodies diluted in blocking solution overnight at 4°C. On the next day, sections were washed with PBS-T and incubated with secondary antibodies for 1 h. Primary antibodies used were anti-CD31 (1:500; BD), anti-pH3 (1:200; EMD Millipore), anti-Ki67 (1:200; Thermo Fisher Scientific), anti-SMM HC (1:100; Biomedical Technologies), anti-fibronectin (1:200; Sigma-Aldrich), anti–collagen IV (1:500; AbD Serotec), anti–integrin β3 (1:200; Abcam), anti–integrin β1 (1:200; EMD Millipore), anti-pFAK (1:100; Cell Signaling Technology), anti-GFP (1:500; Invitrogen), directly conjugated FITC, Cy3 or Cy5 anti-SMA (1:500; Sigma-Aldrich), and biotinylated anti–PDGFR-β (1:50; R&D Systems). For PDGFR-β staining, signal was amplified by using biotin-conjugated antibody, and then aortic sections were incubated with the ABC Elite reagent (Vector Laboratories) and FITC Tyramide reagent (Perkin-Elmer) as described previously (Greif et al., 2012). Staining with the WOW-1 mouse primary antibody (a gift from S. Shattil, University of California, San Diego, La Jolla, CA), which recognizes activated αvβ3 (Pampori et al., 1999), was conducted with the Mouse-on-Mouse Immunodetection kit (Vector Laboratories). The manufacturer's guidelines were followed except sections were incubated with WOW-1 antibody (1:50) overnight at 4°C, washed with PBS-T, and then incubated with directly conjugated secondary antibody. Secondary antibodies were conjugated to either FITC or Alexa Fluor 488, 564, or 647 fluorophores (1:500; Invitrogen). Staining with DAPI (1:1,000) or propidium iodide (1:200) was used to visualize nuclei.

Aortas from patients with SVAS as an isolated entity (15 yr old) or as part of WBS (5 mo old and 46 yr old; Urbán et al., 2002; Pober et al., 2008; Li et al., 2013) and from age-matched human controls were fixed in formalin, paraffin embedded, and sectioned. Paraffin was removed from sections of human aortas with xylene, and after ethanol washes, sections were rehydrated into water. Rehydrated sections were washed with TNT (10 mM Tris-HCl, pH 8.0, 150 mM NaCl, and 0.2% Tween-20) and subjected to antigen retrieval by incubating in boiling 10 mM sodium citrate, pH 6.0, for 20 min. Sections were then immersed in cold water and immunostained as described in the previous paragraph for cryosections except washes were done in TNT.

Fate mapping and clonal analysis. Dams pregnant with *SMA-CreER*^{T2} or *Cdh5-CreER*^{T2} embryos that were heterozygous for a Cre reporter and also null, heterozygous, or wild type for the elastin gene were induced at E12.5 with an intraperitoneal injection of 1.5 mg tamoxifen and 0.75 mg of concomitant progesterone to prevent dystocia. Transverse cryosections (10 µm thick) through the distal thoracic descending aorta were, in the case of *ROSA26R*$^{(mTmG/+)}$ newborns, stained for GFP or, in the case of *ROSA26*$^{(Rb/+)}$ embryos, stained with DAPI and imaged using fluorescent filters for DAPI and the Rb colors (i.e., Cerulean, mOrange, and mCherry).

Pharmacological inhibition of β3 in vivo. Miniature osmotic pumps (flow rate 1 µl/h; Alzet) were loaded with 200 µl of the β3 inhibitor cilengitide (Merck-KgaA; obtained via the National Cancer Institute) at 15 mg/ml in PBS or vehicle alone (PBS). Pumps were then implanted s.c. in dams pregnant with *Eln*$^{(-/-)}$ embryos at E13.5, and pups were euthanized and analyzed at P0.5.

pH3 or Ki67 cell counts. Transverse descending aortic cryosections of wild-type or *Eln*$^{(+/-)}$ embryos at E18.5 and wild-type, *Eln*$^{(-/-)}$, *Itgb3*$^{(+/-)}$*Eln*$^{(-/-)}$, or *Itgb3*$^{(-/-)}$*Eln*$^{(-/-)}$ embryos at E17.5 were stained for the mitotic marker pH3, SMA, CD31, and nuclei (DAPI). Alternatively, wild-type, *Eln*$^{(+/-)}$, and *Eln*$^{(-/-)}$ aortic sections were stained for the proliferation marker Ki67, SMA, and nuclei (propidium iodide). For wild-type and *Eln*$^{(+/-)}$ embryos at E18.5, analysis was limited to aortic sections with five smooth muscle layers, and SMC proliferation was scored by aortic wall position of pH3$^+$ or Ki67$^+$ SMCs, identified as layer 1 (the cell layer adjacent to the ECs), the next radial layer (layer 2), and sequentially outward radially from layers 3–5. For each embryo, the total aortic SMCs per section or layer was estimated by counting and averaging the DAPI$^+$ nuclei of SMCs in four randomly chosen sections. The total number of pH3$^+$ aortic or Ki67$^+$ SMCs per section or layer were counted in 20 sections per embryo.

Quantitative real-time PCR analysis. Descending aortas were dissected from mouse embryos and snap frozen in liquid nitrogen. The RNA of individual aortas of specific *Eln* genotypes was isolated with the RNeasy Plus kit (Life Technologies), and this RNA (0.5 µg) was reverse transcribed with the iScript cDNA Synthesis kit (Bio-Rad Laboratories). Expression levels of selected genes were determined by

quantitative PCR and normalized to *Gapdh*. The following forward and reverse primer pairs were used for these genes (encoded protein): *Acta2* (SMA), 5′-GTCCCAGACATC AGGGAGTAA-3′ and 5′-TCGGATACTTCAGCGTCA GGA-3′; *Tagln* (SM22-α), 5′-CAACAAGGGTCCATC CTACGG-3′ and 5′-ATCTGGGCGGCCTACATCA-3′; *Myh11* (SMMHC), 5′-AAGCTGCGGCTAGAGGTCA-3′ and 5′-CCCTCCCTTTGATGGCTGAG-3′; *Itgb1* (Integrin β1), 5′-CTCCAGAAGGTGGCTTTGATGC-3′ and 5′-GTGAAACCCAGCATCCGTGGAA-3′; *Itgb3* (Integrin β3), 5′-GTGAGTGCGATGACTTCTCCTG-3′ and 5′-CAGGTGTCAGTGCGTGTAGTAC-3′; and *Gapdh* (GAPDH), 5′-CATCACTGCCACCCAGAAGACTG-3′ and 5′-ATGCCAGTGAGCTTCCCGTTCAG-3′.

Quantification of aortic wall parameters. Transverse sections were used for aortic medial wall and lumen quantifications. The medial wall and lumen areas were calculated by measuring the area of SMA staining and the area interior to CD31 staining, respectively.

Nucleus orientation analysis. Threshold images of SMC nuclei (DAPI staining) were used to determine the nuclear centroid and orientation angle (θ_n) with respect to a fixed edge of the entire image. Thresholding of endothelium (CD31 staining) at the aortic lumen boundary was performed, and lumen boundary coordinates were set as the intersection of this boundary with the line joining the centroids of the nucleus and lumen. These coordinates were then used to find the local lumen boundary (arc) orientation angle (θ_{LB}) with respect to the image edge. Finally, nuclear orientation with respect to lumen boundary is given by the angle θ, which is the absolute value of the difference between θ_n and θ_{LB}.

Patient-derived iPSC-SMC generation. Human iPSC-SMCs were generated as described previously (Ge et al., 2012). In brief, epicardial coronary arteries were obtained from explanted hearts of organ donors or recipients of patients with or without SVAS under protocols approved by the Institutional Review Board of Yale University. Isolated SMCs were reprogrammed into iPSC clones, which were expanded, induced to form embryoid bodies, and finally differentiated into SMCs.

Western blot. For protein analysis, iPSC-SMCs were lysed in a RIPA buffer containing complete protease inhibitor and phosSTOP phosphatase inhibitor cocktails (Roche). Lysates were centrifuged at 15,000 rpm for 30 min at 4°C, and supernatants were collected. Protein was separated by SDS-PAGE and transferred to nitrocellulose membranes. Membranes were blocked with 5% BSA in PBS containing 0.05% Tween-20 for 1 h and then incubated with rabbit anti–integrin β3 (1:1,000; Abcam) and rat anti-GAPDH antibodies (1:2,000; Cell Signaling Technology) overnight at 4°C. After washing, membranes were incubated with horseradish peroxidase–conjugated secondary antibodies (1:3,000; Cell Signaling Technology) for 1 h. A Western blotting substrate (ECL Plus; Pierce) and an imaging system (G:Box; Syngene) were used for detection.

Imaging. Fluorescent images were acquired with an upright fluorescence microscope (Eclipse 80i; Nikon) or a confocal microscope (SP5; Leica). For image processing and analysis, cell counting, and nuclear orientation computation, Photoshop (Adobe), ImageJ (National Institutes of Health) software, and custom written programs in MATLAB (R2013a; MathWorks) were used.

Statistical analysis. Student's *t* test or multifactor ANOVA and post hoc test with Bonferroni corrections were used to analyze the data (StatPlus software). All data are presented as mean ± SD.

ACKNOWLEDGMENTS

We thank Greif laboratory members for input. We also thank I. Weissman (Stanford University, Stanford, CA), D. Metzger (Institut Génétique Biologie Moléculaire Cellulaire [IGBMC], Illkirch-Graffenstaden, France), P. Chambon (IGBMC), and D. Li (University of Utah, Salt Lake City, UT) for mouse strains, and S. Shattil for the WOW-1 antibody.

Support was provided by the Brown-Coxe Fellowship from Yale University (A. Misra), the National Institutes of Health (grants R01HL125815 and K08HL093362 to D.M. Greif, R01HL0906485 to Z. Urban, and R01HL116705 to Y. Qyang), the Pulmonary Hypertension Association (the Clinical Scientist Development Award to D.M. Greif), the American Heart Association (Grant-in-Aid 14GRNT19990019 to D.M. Greif), and Connecticut Regenerative Medicine Research (grant 12-SCB-YALE-06 to Y. Qyang).

The authors declare no competing financial interests.

Submitted: 21 April 2015
Accepted: 8 January 2016

REFERENCES

Arciniegas, E., M.G. Frid, I.S. Douglas, and K.R. Stenmark. 2007. Perspectives on endothelial-to-mesenchymal transition: potential contribution to vascular remodeling in chronic pulmonary hypertension. *Am. J. Physiol. Lung Cell. Mol. Physiol.* 293:L1–L8. http://dx.doi.org/10.1152/ajplung.00378.2006

Arjonen, A., R. Kaukonen, and J. Ivaska. 2011. Filopodia and adhesion in cancer cell motility. *Cell Adhes. Migr.* 5:421–430. http://dx.doi.org/10.4161/cam.5.5.17723

Chen, P.Y., L. Qin, C. Barnes, K. Charisse, T.Yi, X. Zhang, R. Ali, P.P. Medina, J. Yu, F.J. Slack, et al. 2012. FGF regulates TGF-β signaling and endothelial-to-mesenchymal transition via control of let-7 miRNA expression. *Cell Reports.* 2:1684–1696. http://dx.doi.org/10.1016/j.celrep.2012.10.021

Choi, E.T., M.F. Khan, J.E. Leidenfrost, E.T. Collins, K.P. Boc, B.R. Villa, D.V. Novack, W.C. Parks, and D.R. Abendschein. 2004. β3-integrin mediates smooth muscle cell accumulation in neointima after carotid ligation in mice. *Circulation.* 109:1564–1569. http://dx.doi.org/10.1161/01.CIR.0000121733.68724.FF

Curran, M.E., D.L. Atkinson, A.K. Ewart, C.A. Morris, M.F. Leppert, and M.T. Keating. 1993. The elastin gene is disrupted by a translocation associated with supravalvular aortic stenosis. *Cell.* 73:159–168. http://dx.doi.org/10.1016/0092-8674(93)90168-P

Dechantsreiter, M.A., E. Planker, B. Mathä, E. Lohof, G. Hölzemann, A. Jonczyk, S.L. Goodman, and H. Kessler. 1999. *N*-Methylated cyclic RGD peptides as highly active and selective $\alpha_V\beta_3$ integrin antagonists. *J. Med. Chem.* 42:3033–3040. http://dx.doi.org/10.1021/jm970832g

DeRuiter, M.C., R.E. Poelmann, J.C. VanMunsteren, V. Mironov, R.R. Markwald, and A.C. Gittenberger-de Groot. 1997. Embryonic

endothelial cells transdifferentiate into mesenchymal cells expressing smooth muscle actins in vivo and in vitro. *Circ. Res.* 80:444–451. http://dx.doi.org/10.1161/01.RES.80.4.444

Feil, S., F. Hofmann, and R. Feil. 2004. SM22α modulates vascular smooth muscle cell phenotype during atherogenesis. *Circ. Res.* 94:863–865. http://dx.doi.org/10.1161/01.RES.0000126417.38728.F6

Ge, X., Y. Ren, O. Bartulos, M.Y. Lee, Z. Yue, K.Y. Kim, W. Li, P.J. Amos, E.C. Bozkulak, A. Iyer, et al. 2012. Modeling supravalvular aortic stenosis syndrome with human induced pluripotent stem cells. *Circulation*. 126:1695–1704. http://dx.doi.org/10.1161/CIRCULATIONAHA.112.116996

Greif, D.M., M. Kumar, J.K. Lighthouse, J. Hum, A. An, L. Ding, K. Red-Horse, F.H. Espinoza, L. Olson, S. Offermanns, and M.A. Krasnow. 2012. Radial construction of an arterial wall. *Dev. Cell*. 23:482–493. http://dx.doi.org/10.1016/j.devcel.2012.07.009

Herring, B.P., A.M. Hoggatt, C. Burlak, and S. Offermanns. 2014. Previously differentiated medial vascular smooth muscle cells contribute to neointima formation following vascular injury. *Vasc. Cell*. 6:21. http://dx.doi.org/10.1186/2045-824X-6-21

Hodivala-Dilke, K.M., K.P. McHugh, D.A. Tsakiris, H. Rayburn, D. Crowley, M. Ullman-Culleré, F.P. Ross, B.S. Coller, S. Teitelbaum, and R.O. Hynes. 1999. β3-integrin–deficient mice are a model for Glanzmann thrombasthenia showing placental defects and reduced survival. *J. Clin. Invest*. 103:229–238. http://dx.doi.org/10.1172/JCI5487

Hoshiga, M., C.E. Alpers, L.L. Smith, C.M. Giachelli, and S.M. Schwartz. 1995. $\alpha_V\beta_3$ integrin expression in normal and atherosclerotic artery. *Circ. Res.* 77:1129–1135. http://dx.doi.org/10.1161/01.RES.77.6.1129

Karnik, S.K., B.S. Brooke, A. Bayes-Genis, L. Sorensen, J.D. Wythe, R.S. Schwartz, M.T. Keating, and D.Y. Li. 2003. A critical role for elastin signaling in vascular morphogenesis and disease. *Development*. 130:411–423. http://dx.doi.org/10.1242/dev.00223

Lawler, J., R. Weinstein, and R.O. Hynes. 1988. Cell attachment to thrombospondin: the role of ARG-GLY-ASP, calcium, and integrin receptors. *J. Cell Biol*. 107:2351–2361. http://dx.doi.org/10.1083/jcb.107.6.2351

Li, D.Y., B. Brooke, E.C. Davis, R.P. Mecham, L.K. Sorensen, B.B. Boak, E. Eichwald, and M.T. Keating. 1998a. Elastin is an essential determinant of arterial morphogenesis. *Nature*. 393:276–280. http://dx.doi.org/10.1038/30522

Li, D.Y., G. Faury, D.G. Taylor, E.C. Davis, W.A. Boyle, R.P. Mecham, P. Stenzel, B. Boak, and M.T. Keating. 1998b. Novel arterial pathology in mice and humans hemizygous for elastin. *J. Clin. Invest*. 102:1783–1787. http://dx.doi.org/10.1172/JCI4487

Li, W., Q. Li, L. Qin, R. Ali, Y. Qyang, M. Tassabehji, B.R. Pober, W.C. Sessa, F.J. Giordano, and G. Tellides. 2013. Rapamycin inhibits smooth muscle cell proliferation and obstructive arteriopathy attributable to elastin deficiency. *Arterioscler. Thromb. Vasc. Biol*. 33:1028–1035. http://dx.doi.org/10.1161/ATVBAHA.112.300407

Maile, L.A., W.H. Busby, T.C. Nichols, D.A. Bellinger, E.P. Merricks, M. Rowland, U. Veluvolu, and D.R. Clemmons. 2010. A monoclonal antibody against $\alpha_V\beta_3$ integrin inhibits development of atherosclerotic lesions in diabetic pigs. *Sci. Transl. Med*. 2:18ra11. http://dx.doi.org/10.1126/scitranslmed.3000476

Miano, J.M., P. Cserjesi, K.L. Ligon, M. Periasamy, and E.N. Olson. 1994. Smooth muscle myosin heavy chain exclusively marks the smooth muscle lineage during mouse embryogenesis. *Circ. Res.* 75:803–812. http://dx.doi.org/10.1161/01.RES.75.5.803

Morimoto, M., Z. Liu, H.T. Cheng, N. Winters, D. Bader, and R. Kopan. 2010. Canonical Notch signaling in the developing lung is required for determination of arterial smooth muscle cells and selection of Clara versus ciliated cell fate. *J. Cell Sci*. 123:213–224. http://dx.doi.org/10.1242/jcs.058669

Muzumdar, M.D., B. Tasic, K. Miyamichi, L. Li, and L. Luo. 2007. A global double-fluorescent Cre reporter mouse. *Genesis*. 45:593–605. http://dx.doi.org/10.1002/dvg.20335

Owens, G.K., M.S. Kumar, and B.R. Wamhoff. 2004. Molecular regulation of vascular smooth muscle cell differentiation in development and disease. *Physiol. Rev.* 84:767–801. http://dx.doi.org/10.1152/physrev.00041.2003

Pampori, N., T. Hato, D.G. Stupack, S. Aidoudi, D.A. Cheresh, G.R. Nemerow, and S.J. Shattil. 1999. Mechanisms and consequences of affinity modulation of integrin $\alpha_V\beta_3$ detected with a novel patch-engineered monovalent ligand. *J. Biol. Chem*. 274:21609–21616. http://dx.doi.org/10.1074/jbc.274.31.21609

Pober, B.R., M. Johnson, and Z. Urban. 2008. Mechanisms and treatment of cardiovascular disease in Williams-Beuren syndrome. *J. Clin. Invest*. 118:1606–1615. http://dx.doi.org/10.1172/JCI35309

Qiao, L., T. Nishimura, L. Shi, D. Sessions, A. Thrasher, J.R. Trudell, G.J. Berry, R.G. Pearl, and P.N. Kao. 2014. Endothelial fate mapping in mice with pulmonary hypertension. *Circulation*. 129:692–703. http://dx.doi.org/10.1161/CIRCULATIONAHA.113.003734

Raines, E.W., and R. Ross. 1993. Smooth muscle cells and the pathogenesis of the lesions of atherosclerosis. *Br. Heart J.* 69(1 Suppl):S30–S37. http://dx.doi.org/10.1136/hrt.69.1_Suppl.S30

Ranchoux, B., F. Antigny, C. Rucker-Martin, A. Hautefort, C. Péchoux, H.J. Bogaard, P. Dorfmüller, S. Remy, F. Lecerf, S. Planté, et al. 2015. Endothelial-to-mesenchymal transition in pulmonary hypertension. *Circulation*. 131:1006–1018. http://dx.doi.org/10.1161/CIRCULATIONAHA.114.008750

Rinkevich, Y., P. Lindau, H. Ueno, M.T. Longaker, and I.L. Weissman. 2011. Germ-layer and lineage-restricted stem/progenitors regenerate the mouse digit tip. *Nature*. 476:409–413. http://dx.doi.org/10.1038/nature10346

Sandberg, L.B., N.T. Soskel, and J.G. Leslie. 1981. Elastin structure, biosynthesis, and relation to disease states. *N. Engl. J. Med*. 304:566–579. http://dx.doi.org/10.1056/NEJM198103053041004

Scheppke, L., E.A. Murphy, A. Zarpellon, J.J. Hofmann, A. Merkulova, D.J. Shields, S.M. Weis, T.V. Byzova, Z.M. Ruggeri, M.L. Iruela-Arispe, and D.A. Cheresh. 2012. Notch promotes vascular maturation by inducing integrin-mediated smooth muscle cell adhesion to the endothelial basement membrane. *Blood*. 119:2149–2158. http://dx.doi.org/10.1182/blood-2011-04-348706

Schneider, J.G., Y. Zhu, T. Coleman, and C.F. Semenkovich. 2007. Macrophage β3 integrin suppresses hyperlipidemia-induced inflammation by modulating TNFα expression. *Arterioscler. Thromb. Vasc. Biol*. 27:2699–2706. http://dx.doi.org/10.1161/ATVBAHA.107.153650

Seidelmann, S.B., J.K. Lighthouse, and D.M. Greif. 2014. Development and pathologies of the arterial wall. *Cell. Mol. Life Sci*. 71:1977–1999. http://dx.doi.org/10.1007/s00018-013-1478-y

Shankman, L.S., D. Gomez, O.A. Cherepanova, M. Salmon, G.F. Alencar, R.M. Haskins, P. Swiatlowska, A.A. Newman, E.S. Greene, A.C. Straub, et al. 2015. KLF4-dependent phenotypic modulation of smooth muscle cells has a key role in atherosclerotic plaque pathogenesis. *Nat. Med*. 21:628–637. http://dx.doi.org/10.1038/nm.3866

Sheikh, A.Q., J.K. Lighthouse, and D.M. Greif. 2014. Recapitulation of developing artery muscularization in pulmonary hypertension. *Cell Reports*. 6:809–817. http://dx.doi.org/10.1016/j.celrep.2014.01.042

Sheikh, A.Q., A. Misra, I.O. Rosas, R.H. Adams, and D.M. Greif. 2015. Smooth muscle cell progenitors are primed to muscularize in pulmonary hypertension. *Sci. Transl. Med*. 7:308ra159. http://dx.doi.org/10.1126/scitranslmed.aaa9712

Shifren, A., A.G. Durmowicz, R.H. Knutsen, E. Hirano, and R.P. Mecham. 2007. Elastin protein levels are a vital modifier affecting normal lung development and susceptibility to emphysema. *Am. J. Physiol. Lung*

Cell. Mol. Physiol. 292:L778–L787. http://dx.doi.org/10.1152/ajplung.00352.2006

Stouffer, G.A., Z. Hu, M. Sajid, H. Li, G. Jin, M.T. Nakada, S.R. Hanson, and M.S. Runge. 1998. β_3 integrins are upregulated after vascular injury and modulate thrombospondin- and thrombin-induced proliferation of cultured smooth muscle cells. *Circulation.* 97:907–915. http://dx.doi.org/10.1161/01.CIR.97.9.907

Streuli, C.H. 2009. Integrins and cell-fate determination. *J. Cell Sci.* 122:171–177. http://dx.doi.org/10.1242/jcs.018945

Stupp, R., M.E. Hegi, T. Gorlia, S.C. Erridge, J. Perry, Y.K. Hong, K.D. Aldape, B. Lhermitte, T. Pietsch, D. Grujicic, et al. CENTRIC Study Team. 2014. Cilengitide combined with standard treatment for patients with newly diagnosed glioblastoma with methylated MGMT promoter (CENTRIC EORTC 26071-22072 study): a multicentre, randomised, open-label, phase 3 trial. *Lancet Oncol.* 15:1100–1108. http://dx.doi.org/10.1016/S1470-2045(14)70379-1

Urbán, Z., S. Riazi, T.L. Seidl, J. Katahira, L.B. Smoot, D. Chitayat, C.D. Boyd, and A. Hinek. 2002. Connection between elastin haploinsufficiency and increased cell proliferation in patients with supravalvular aortic stenosis and Williams-Beuren syndrome. *Am. J. Hum. Genet.* 71:30–44. http://dx.doi.org/10.1086/341035

Wagenseil, J.E., C.H. Ciliberto, R.H. Knutsen, M.A. Levy, A. Kovacs, and R.P. Mecham. 2009. Reduced vessel elasticity alters cardiovascular structure and function in newborn mice. *Circ. Res.* 104:1217–1224. http://dx.doi.org/10.1161/CIRCRESAHA.108.192054

Wagenseil, J.E., C.H. Ciliberto, R.H. Knutsen, M.A. Levy, A. Kovacs, and R.P. Mecham. 2010. The importance of elastin to aortic development in mice. *Am. J. Physiol. Heart Circ. Physiol.* 299:H257–H264. http://dx.doi.org/10.1152/ajpheart.00194.2010

Wang, Y., M. Nakayama, M.E. Pitulescu, T.S. Schmidt, M.L. Bochenek, A. Sakakibara, S. Adams, A. Davy, U. Deutsch, U. Lüthi, et al. 2010. Ephrin-B2 controls VEGF-induced angiogenesis and lymphangiogenesis. *Nature.* 465:483–486. http://dx.doi.org/10.1038/nature09002

Wendling, O., J.M. Bornert, P. Chambon, and D. Metzger. 2009. Efficient temporally-controlled targeted mutagenesis in smooth muscle cells of the adult mouse. *Genesis.* 47:14–18. http://dx.doi.org/10.1002/dvg.20448

Weng, S., L. Zemany, K.N. Standley, D.V. Novack, M. La Regina, C. Bernal-Mizrachi, T. Coleman, and C.F. Semenkovich. 2003. β3 integrin deficiency promotes atherosclerosis and pulmonary inflammation in high-fat-fed, hyperlipidemic mice. *Proc. Natl. Acad. Sci. USA.* 100:6730–6735. http://dx.doi.org/10.1073/pnas.1137612100

Yamashita, J., H. Itoh, M. Hirashima, M. Ogawa, S. Nishikawa, T. Yurugi, M. Naito, K. Nakao, and S. Nishikawa. 2000. Flk1-positive cells derived from embryonic stem cells serve as vascular progenitors. *Nature.* 408:92–96. http://dx.doi.org/10.1038/35040568